Water Monolayers: An Overlooked Loss Mechanism in Mid-Infrared Photonics – Supplement

Antonia Torres-Cubillo,[1,2] Martin Feiler,[1,3] Roman Zakoldaev,[1] Jehona Salaj,[1] Noémie Mestre,[1] Sebastián Alberti,[1] Henock D. Yallwe,[1] and Jana Jágerská[1]

[1)] *UiT The Arctic University of Norway, NO-9037 Tromsø, Norway*

[2)] *University of Málaga, 29010 Málaga, Spain*

[3)] *Slovak University of Technology in Bratislava, 81219 Bratislava, Slovakia*

S1. WAVEGUIDE GEOMETRIES

The slot waveguide, whose schematic cross section and top view can be observed in Fig. S1(a), was designed for methane detection at $\lambda = 3.27\,\mu\text{m}$ on a silicon-on-insulator (SOI) platform and is described in[1]. The designed dimensions are $H = 500\,\text{nm}$, $W = 550\,\text{nm}$, $s = 150\,\text{nm}$. The buried-oxide (BOX) layer has a thickness $H_{\text{BOX}} = 3\,\mu\text{m}$. The geometry of the silicon nitride (SiN) suspended waveguide with micro-structured lateral cladding is illustrated in Fig. S1(b). The sample designed at $\lambda = 3.27\,\mu\text{m}$ is a W3 waveguide, with lattice period $a = 1.3\,\mu\text{m}$ and hole diameter $d = 1.1\,\mu\text{m}$, whereas the one working at $\lambda = 4.35\,\mu\text{m}$ is a W5 featuring $a = 2\,\mu\text{m}$ and $d = 1.55\,\mu\text{m}$[2]. In both cases, the thicknesses of the guiding layer and the undercut are $H = 500\,\text{nm}$ and $H_{\text{u}} > 30\,\mu\text{m}$, respectively.

Representative SEM images of the SOI slot and the SiN suspended waveguide are shown in Fig. S2(a)–(b). By analyzing the picture of the slot waveguide (Fig. S2(a)), several deviations from the ideal geometry are observed, including over-etching down to the BOX layer, and slightly angled Si sidewalls, resulting in narrowing of the slot towards the bottom of the structure. These are accounted for in the waveguide model we describe in Sec. S4.

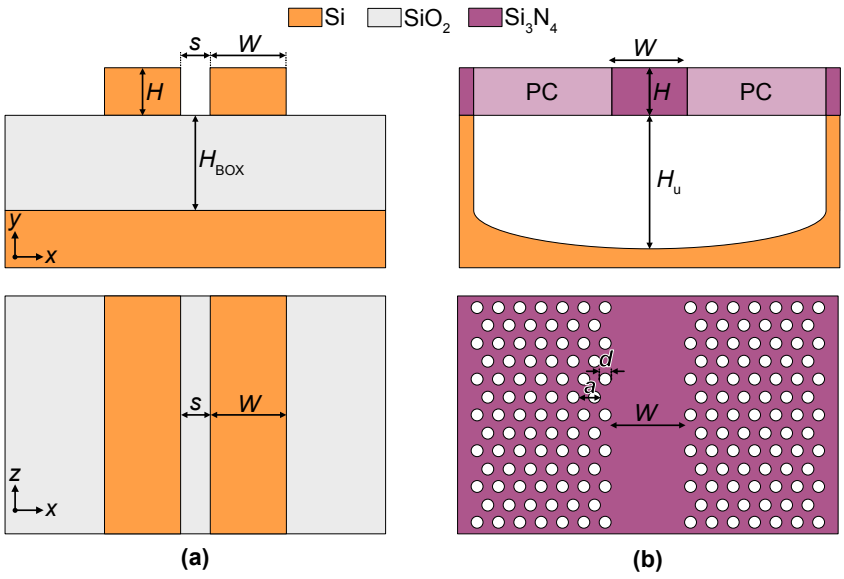

FIG. S1. Schematic cross-sectional and top views of the (a) silicon slot and (b) silicon nitride suspended waveguides analyzed in this work. Note that the representations are not at true scale.

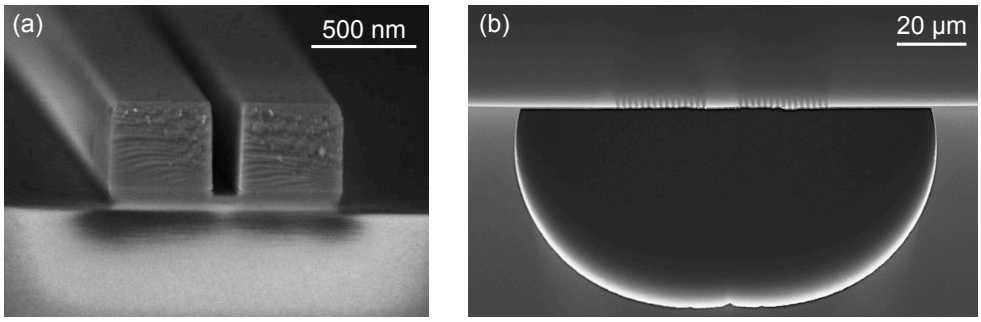

FIG. S2. SEM pictures of the (a) silicon slot and (b) silicon nitride suspended waveguides.

S2. EXTENDED EXPERIMENTAL DATA

Figure S3 shows a representative time-resolved measurement of the slot-waveguide loss, with the corresponding relative humidity (RH) color-encoded. At each RH step, we acquired multiple traces that capture the approach to a local steady state. As shown in the inset, the loss values at a given set point are well described by an exponential model. For our analysis, we used, at each RH set point, the value obtained by extrapolating the exponential fit to 99% of the steady-state response. This choice removes minor artifacts due to small variations in acquisition timing across steps. The discrepancy between the last recorded point and the extrapolated saturation value is small ($< 2\%$ of the value), indicating that the extrapolation introduces negligible bias.

Figure S4 presents the full set of excess-loss measurements for both the slot and suspended waveguides, with vertical scales adjusted to the respective data ranges. Repeated measurements were performed for the slot waveguide to assess the repeatability of the procedure and reproducibility of the results, yielding a standard deviation of only $\sigma \approx 0.17\,\mathrm{dB/cm}$. The same experimental protocol was applied to the SiN membrane waveguides, lending confidence to the consistency of the results.

S3. CONTACT-ANGLE MEASUREMENTS

To assess the wettability of the investigated material surfaces, sessile drop measurements were performed directly on the fabricated chips, as close as possible to the waveguide structures. A deionised water droplet with a volume of 7 µl was deposited using a pipette positioned approximately 2.5 mm above the surface. The results, shown in Fig. S5, indicate

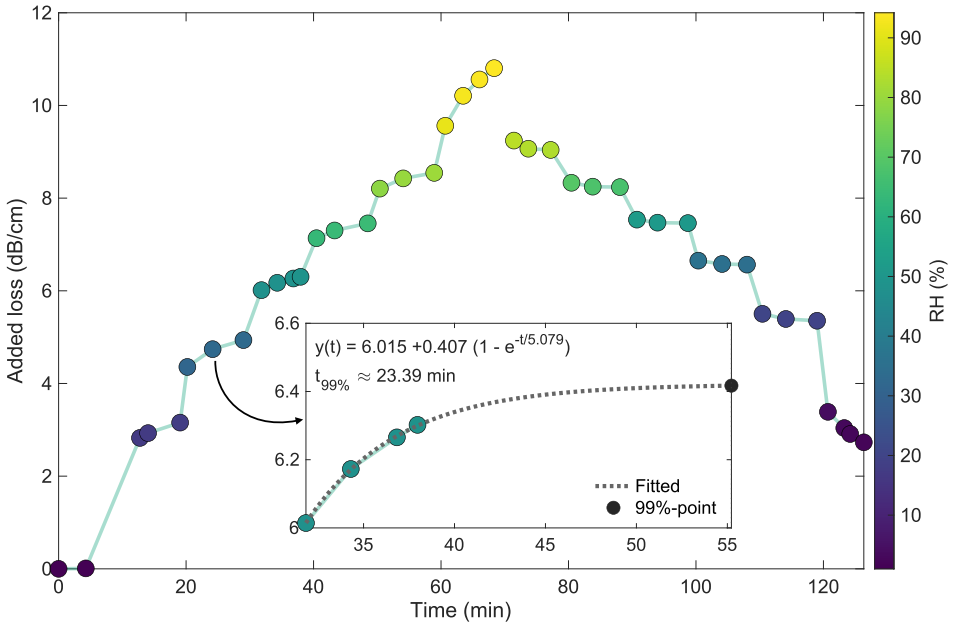

FIG. S3. Time-resolved measurements of the slot waveguide. Relative humidity is color-encoded. The inset shows the exponential model fitted to the loss values within one step.

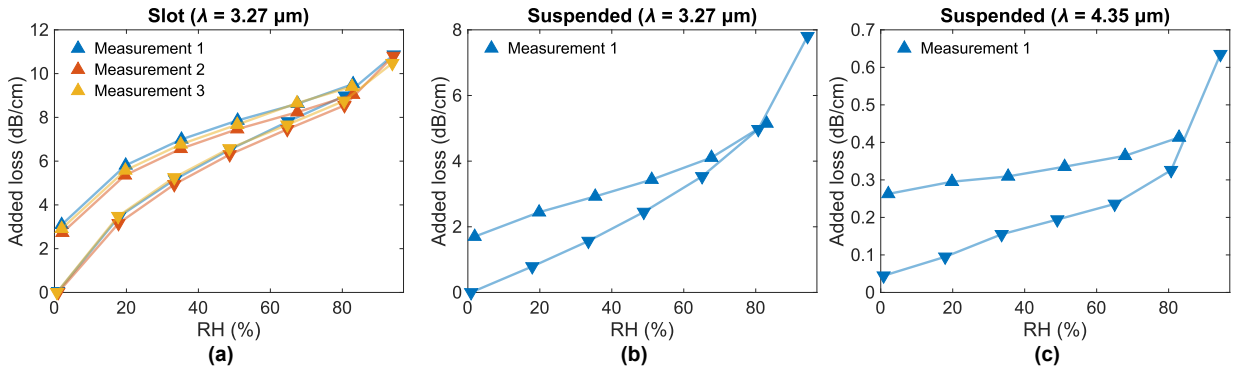

FIG. S4. Complete set of measurements of the (a) slot and (b,c) suspended waveguides, operating at (b) $\lambda = 3.27\,\mu$m and (c) $\lambda = 4.35\,\mu$m. Good measurement repeatability is evident from the slot results.

that silicon exhibits strongly hydrophobic behaviour, with an average contact angle of 94.2° across different measurements. Silicon nitride, in contrast, is moderately hydrophobic, with an average contact angle of 65.1°. As a reference, measurements on a SiO_2 glass slide show significantly higher hydrophilicity, with an average contact angle of 40.4°, in good agreement with literature values and markedly lower than those of Si and SiN[3,4]. It should be

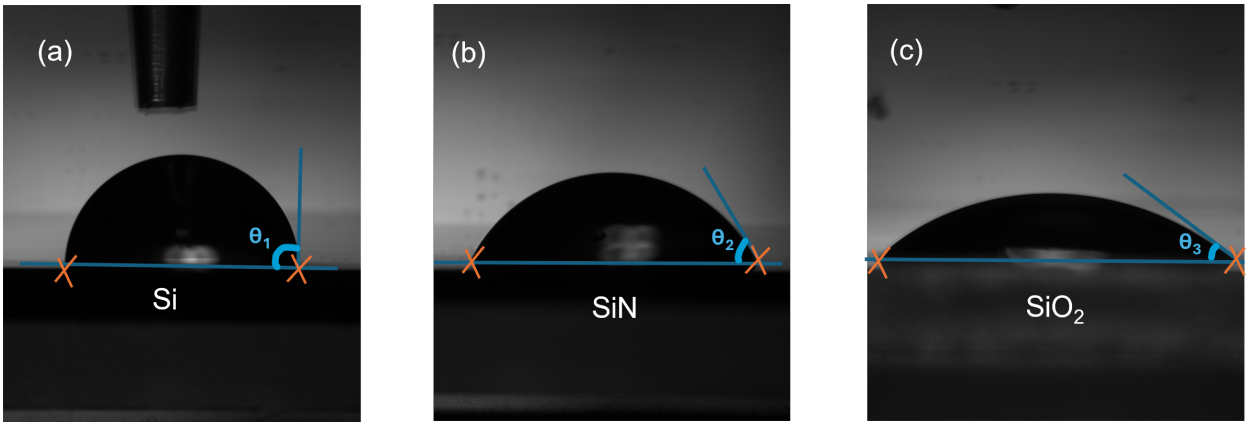

FIG. S5. Representative side-view images of water droplets deposited on (a) Si, (b) SiN, and (c) SiO_2 surfaces for contact angle analysis. The baseline and tangent at the three-phase contact point are used to determine the contact angle θ, as illustrated. Variations in the measured angles $\theta_1 = 94°$, $\theta_2 = 65°$, and $\theta_3 = 40°$ reflect differences in surface wettability.

noted that this technique probes only the top surface of the chips; the wettability of vertical sidewalls and buried interfaces is inferred from the fabrication processes.

S4. SIMULATION DETAILS

Figure S6(a) shows the modeled slot waveguide cross-section used in the numerical simulations (Ansys Lumerical), incorporating the main fabrication deviations observed in SEM

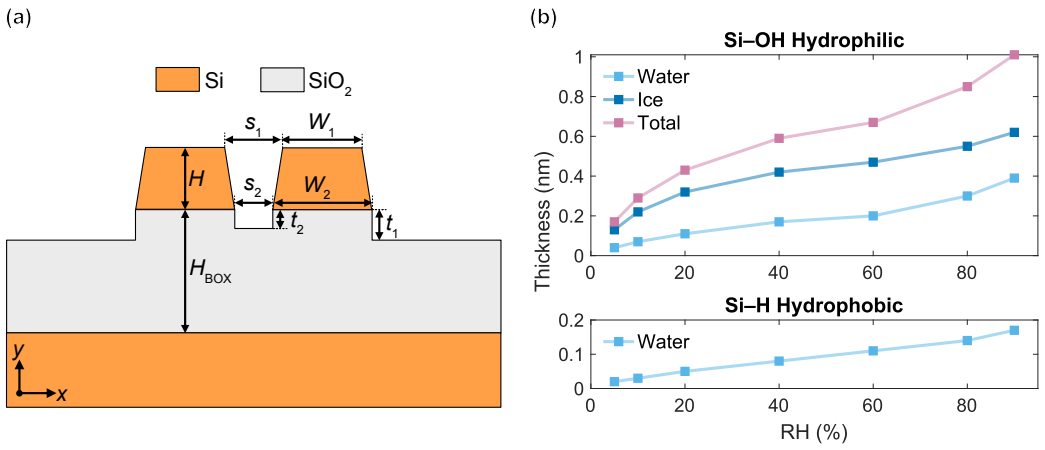

FIG. S6. (a) Slot waveguide cross section as modelled in numerical simulations. (b) Model for the adsorbed water layers employed in simulations based on data published in Ref.[5].

images, such as the example in Fig. S2(a). Based on this analysis, the following dimensions were used: $W_1 = 550\,\text{nm}$, $W_2 = 560\,\text{nm}$, $s_1 = 150\,\text{nm}$, $s_2 = 140\,\text{nm}$, $t_1 = 100\,\text{nm}$, and $t_2 = 30\,\text{nm}$. The total silicon and buried oxide thicknesses were kept at $H = 500\,\text{nm}$ and $H_{\text{BOX}} = 3\,\mu\text{m}$, respectively.

To model humidity effects, ice- and liquid-like water layers were introduced on all air-exposed surfaces. The structure and thickness of these layers as a function of relative humidity as extracted from[5] is reproduced in Fig. S6(b).

REFERENCES

[1]H. D. Yallew, M. Vlk, A. Datta, S. Alberti, R. A. Zakoldaev, J. Høvik, A. Aksnes, and J. Jágerská, "Sub-ppm methane detection with mid-infrared slot waveguides," ACS photonics **10**, 4282–4289 (2023).

[2]J. Salaj, M. Vlk, R. Zakoldaev, R. Seton, J. Čtyrokỳ, S. Alberti, A. Aksnes, and J. Jágerská, "Suspended nanophotonic waveguide for isotope-specific CO2 detection," Optica **11**, 1654–1662 (2024).

[3]G. J. Pietsch, En"Hydrogen on Si: Ubiquitous surface termination after wet-chemical processing," Applied Physics A **60**, 347–363 (1995), publisher: Springer.

[4]H. Barhoumi, A. Maaref, and N. Jaffrezic-Renault, "Experimental Study of Thermodynamic Surface Characteristics and pH Sensitivity of Silicon Dioxide and Silicon Nitride," Langmuir **26**, 7165–7173 (2010), publisher: American Chemical Society.

[5]L. Chen, X. He, H. Liu, L. Qian, and S. H. Kim, "Water adsorption on hydrophilic and hydrophobic surfaces of silicon," The Journal of Physical Chemistry C **122**, 11385–11391 (2018).